Power-Aware Improvement in Signal Detection

Scott D. Briles Ph.D (505) 667-4298 briles@lanl.gov
Patrick Shriver (505) 665-0249 pshriver@lanl.gov
Maya Gokhale Ph.D. (505) 665-9095 maya@lanl.gov
Jayashree Harikuma Ph.D (505) 665-9108 jharikumar@lanl.gov

Los Alamos National Laboratory
Space Data Systems Group, NIS-3
Mail Stop D440
Los Alamos, NM 87545

ABSTRACT

Improvements in signal detection characteristics for a remote-sensing instrument can be achieved at the expense of computational effort and the power associated with that effort. DSP used in remote sensing scenarios usually involves the detection of a signal and the estimation of parameters associated with that signal. Fortunately, the algorithms used for parameter estimation are the same algorithms that, through post-processing decision making, decrease the false alarm rate. This post processing allows for the reduction in the false alarm rate as seen at the end product of the instrument. The level of false alarm reduction must be balanced against the amount of additional power that is needed to produce this level. This paper will present quantitative results that demonstrate this tradeoff for a specific application.

This paper focuses on the detection of transient radio frequency (RF) events (e.g., lighting) as observed from the FORTÉ satellite. However, the methodology presented for power-aware improvement in signal detection is general enough to be applied to most remote-sensing scenarios. A suite of algorithms, which vary widely in their precision of estimated parameters, is presented in the paper. Equally wide in variation is the amount of power required by each of the algorithms. Power requirements of the algorithms were obtained by actual physical measurement for a mimic of a RAD750 processor. Algorithm performance was determined via Monte Carlo testing. Using that same Monte Carlo testing post-processing, thresholds for each of the algorithms were developed for the reduction of the false alarm rate. A quantitative display of how each of the algorithms decreases the false alarm rate over the front-end analog detection is displayed versus the power required

Categories and Subject Descriptors

D.3.3 [**Military/Aerospace**]:– *power aware computing.*

General Terms

Algorithms, Measurement, Performance

Keywords

Signal Detection, Power Award Computing

1. INTRODUCTION

The Defense Advanced Research Projects Agency (DARPA) has supported the Los Alamos National Laboratory (LANL) Power Aware Computing and Communications (PAC/C) [1] team to develop an advanced signal processing payload concept derived from the joint LANL and Sandia National Laboratory FORTÉ satellite mission. The objective has been to develop an intelligent payload system that processes received RF lightning signal data onboard the spacecraft in a power-aware manner [2]. The signal-processing tasks include detection and parameter estimation.

The desired receiver performance point of 100% probability of detection and 0% probability of false alarm is not obtainable, but improvements can be made via post-processing at the cost of power usage. Evaluation of the results from the parameter estimation algorithms can be used to improved detection performance through expenditure of energy.

The idea of Algorithm Power Modulation (APM) is intended to be used, where, a signal-processing algorithm is chosen, from a suite of four algorithms, to execute based on the available power, incoming event rate, and algorithm properties. Each signal-processing algorithm has an associated energy consumption and accuracy level which defines the decision trade space. The payload is thus capable of processing data at varying levels or modes of operation as dictated by the current state.

2. BACKGROUND

For this work, we have focused on power-aware processing for a remote-sensing application similar in nature to the mission of FORTÉ. The FORTÉ satellite was launched in August of 1997 and carries a suite of instruments used for studying the optical and RF signals from lightning in the Earth's atmosphere. The results from FORTÉ have led to a better understanding of the relationship between optical and RF lightning events, and future satellite missions can even use this knowledge to help provide global lightning and severe-storm monitoring [3]. The processing algorithms for the RF lightning signals have been chosen in this study.

2.1 Ionospheric-Dispersed Signals

A RF lightning event in the Earth's atmosphere generates a dispersed signal in the VHF spectral region. The dispersion is such that low frequencies of the signal are delayed, as it propagates through the ionosphere. This is known as a "chirp" signal. A simulated chirp signal is shown by the graph in Figure 1. The graph is an illustration of the time-domain signal where frequency decreases with increased time.

The time taken for a given frequency of the chirp signal to arrive at the on-orbit receiver is related to the total electron content (TEC) of the ionosphere along the direction of the signal travel, the given frequency, and the signal time-of-arrival if ionospheric dispersion did not exist [4].

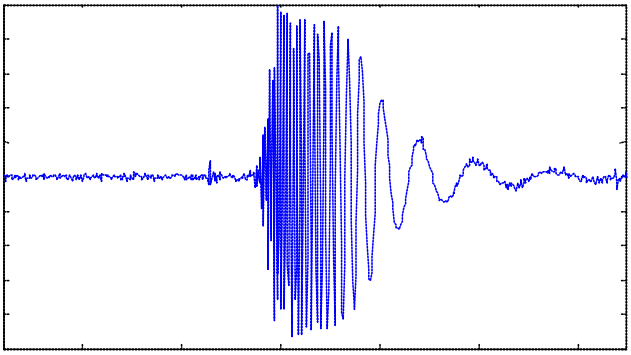

Figure 1. Time vs. Amplitude Profile of Chirp

The total electron content (TEC) represents the number of electrons in a unit-area cross-section of an ionospheric column along the signal path. This atmospheric property is related to the propagation of radio signals through the ionosphere that can distort or bend the signals over the horizon. TEC is also related to the surface temperature of the Earth, and thus, could be viewed as an indicator for storm severity.

2.2 FORTÉ RF Hardware

FORTÉ receives RF signals either from two orthogonal monopoles mounted at the satellite's base or by passive moderate-gain antennas mounted on a 35-foot nadir-directed boom [5]. There are two types of receivers tunable in 30-300 MHz bands, which consist of a mixer, bandpass filter, and a second mixer stage. The first mixer up-converts the antenna signal to a higher frequency then passes the signal through the bandpass filter. The second mixer then converts the band-limited signal to baseband. Depending on the type of receiver, either a 12-bit high-speed digitizer or an 8-bit digitizer is used. The digitizers are in constant operation. An analog trigger box processes the output from the second-stage mixer and determines whether or not the digitized data is to be recorded in payload memory. The recorded data can then be down linked. Data analysis is carried out as part of the ground operation at LANL. Figure 2 shows a conceptual block diagram of the RF hardware.

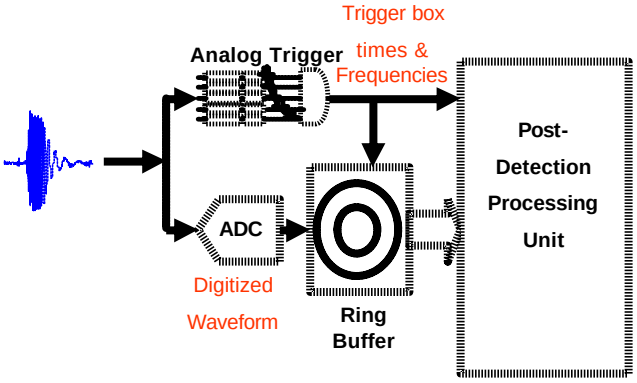

Figure 2. Detection and Data Acquisition Hardware

The analog trigger box detects or rejects incoming signals based on double-threshold channel settings. The analog signal is passed into frequency-separated channels through a set of bandpass filters in the trigger box. Each of the eight channels has an analog trigger associated with it. Once the signal present in the channel causes the threshold to be broken, detection in the channel is declared. A detection is not declared until M $(1 \le M \le 8)$ channels exceed threshold. This double threshold detection scheme produces better detection characteristics than that of a single channel alone. Harrington's method was used to determine the optimal in-channel thresholds for a given signal-to-noise ratio [6]. Figure 3 shows the receiver operating characteristic (ROC) curves for the simulated hardware of this paper. Both continuous and discrete curves of the figure were derived from closed-form analytical solutions.

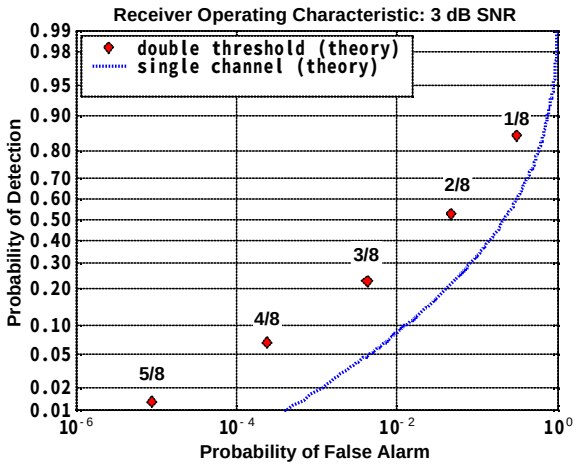

Figure 3. Detection Performance of Analog Trigger Box

For a detection, two sets of data are generated by the parameter estimation algorithms. First, the time of each channel's detection is logged. The center frequency of each bandpass filter can be paired with these time values. This set of data yields a time history of when different frequencies of the chirp signal arrived at the satellite. For the chirp signal, the highest frequency should arrive first then the next highest frequency should arrive and so on. The function associated with these arrival times should be nonlinear in nature [4]. The second set of data yielded by full-signal detect is the digitized time-domain waveform. These two sets of data can be processed to estimate the value of TEC and

further more the estimate of TEC can be used to reduce false alarms.

Unfortunately LANL failed to field any capability for on-orbit processing of the data sets. An instrument known as the FORTÉ Event Classifier was developed and installed aboard the FORTÉ satellite. The mission of the Event Classifier instrument was to implement on-orbit digital signal processing algorithms that could be obtained from either an onboard library or uplink from the ground. However, the Event Classifier was never fully operational at launch and was turned on for testing only one time after launch [5]. Thus the Event Classifier instrument failed to provide any means for testing of new algorithms or concepts on orbit. Therefore the work of this paper does not involve space-based implementations.

2.3 Algorithms

Four algorithms are available to operate on the data in order to yield an estimate of the TEC value. The four algorithms will be referred to as: 1) least-mean-squares (LMS), 2) maximum-likelihood (ML), 3) software trigger box (ST), and 4) match-filter bank (MF). Using only the time-frequency data pairs provided by the channels of the analog trigger box, the first two algorithms use curve-fitting techniques. While the LMS is a deterministic algorithm, the ML is forced to be deterministic by only allowing for 20 iterations to be performed [7]. The remaining two algorithms make use of the 2048-sample, 12-bit, digitized waveform data.

Using digitized waveform data, the software trigger box algorithm utilizes frequency domain processing to provide an estimate of TEC. The software trigger box algorithms first transforms the time-domain data into a non-overlap spectrogram composed of boxcar-windowed, 32-sample FFTs. Upon determining the associated time indexes for the maximums of each of the seventeen non-negative frequency bins, a maximum likelihood algorithm is performed on the data pairs constructed from the bin-maximum times and the center frequencies of the FFT bins.

The MF algorithm also utilizes frequency-domain processing. By generating simulated exemplar time-domain waveforms of different TEC and transforming them into the frequency domain, a bank of match filter can be constructed that spans the space of possible TEC values. A correlation peak is rendered by performing a fast correlation algorithm on the waveform data and a TEC-specific filter. Exploration of the match filter bank for the greatest correlation-peak value is done with a "focus-in" decision tree so that only ten fast correlations are performed to yield an estimate of TEC. However, since the value of the winning peak is not quantized or hard constrained like the TEC estimate, this peak value will be used for post-processing detection work in this paper for the match-filter bank algorithm.

2.4 Power Measurements

Power usage measurements for the four algorithms were obtained through experiments conducted on a 266-MHz PowerPC 750 microprocessor running the VxWorks™ operating system. Both time-to-execute values and power usage estimates (RMS and peak current) were determined for the PowerPC 750. The time-to-execute values are average values over a test set of 21 trials cycled 20 to 100 times. Each trial used synthetically generated data that simulated a chirp-signal event being received by a space-base receiver system containing an analog trigger box and a waveform digitizer.

Table 1. Power Measurements for PowerPC 750

Algorithm	Current (amps-peak)	Execution Time	Energy (Joules)
Least Mean Squares	2.06	3.4 µs	18.7e-6
Maximum Likelihood	2.06	183 µs	1.02e-3
Software Trigger Box	2.18	8.34 ms	47.3e-3
Match Filter Bank	2.04	470 ms	2.35

Power usage for the PowerPC 750 executing the benchmaking code is presented in Table 1. The Jet Propulsion Laboratory (JPL) power-aware testbed consists of a Wind River PPC750 266-MHz processor board that is running VxWorks 5.4.2. The processor operates at a constant 2.67V and current consumption is measured with a Tektronix TDS 7104 Digital Phosphor Oscilloscope. Current is sampled with the Tektronix TCP202 probe that is wired to the board. Software compilation is done with a VxWorks Tornado 2.0.2 programming tools which uses the GNU C compiler.

The software is compiled and downloaded to the testbed with the Tornado target server shell. The programs are run until an "average" current signal snapshot is taken with the oscilloscope. The "average" signal is determined manually by watching the current response during several program runs. The snapshot is taken when the current response produces a fairly consistent signal and consistent measurement value.

2.5 Post-Processing Detection

The output of the four algorithms can be compared against unique thresholds to determine if a false alarm has been generated by the analog trigger box. Figure 4 shows the concept expressed in terms of its effect on the ROC curve. Of course, lost detections can not be corrected for in post processing since the analog trigger box cues the collection of data and the execution of the algorithms. Unique thresholds for each algorithm are needed since the algorithms arrive at their results differently and to the point of this paper, require different amounts of power to obtain those results.

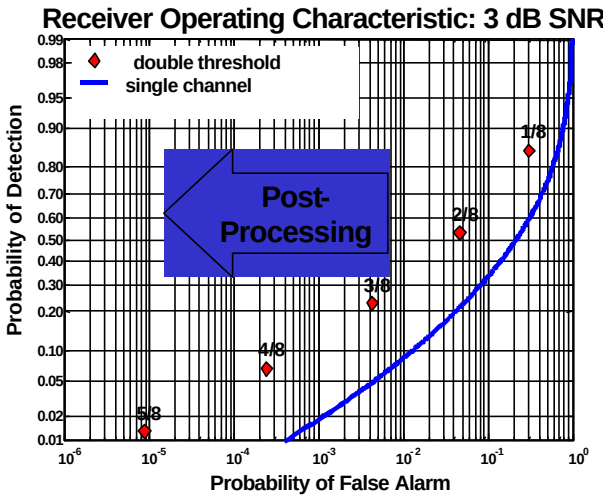

Figure 4. Post-Processing Effect on ROC Curve

3. DATA CREATION

Using computer simulation and Monte Carlo experimentation, the data needed to derive post-processing thresholds and an estimate of performance of the thresholds can be created. Parameters needed for the receiver simulation include the signal-to-noise ratio (SNR) and analog trigger box thresholds, both single channel amplitude thresholds and a binary threshold. For the Monte Carlo experiment, knowledge of the expected probability of detection and probability of false alarm aid in the selection of the number of trials. Once parameters are specified, data is created by exercising a receiver simulation and placing the results of the algorithms in the appropriate logging array. A parameter-estimation algorithm results are separated between a logging array that collects results for a true detect and a logging array that collects results for a false alarm. The conditions of detect and false alarm related to the decision made by the analog trigger box. Thus for each trial of the Monte Carlo experiment, if the simulation provides a detect or a false alarm, data is logged for each algorithm. It should be pointed out that not every trial will produce logged data since conditions of missed detections and proper rejection are not logged.

For a truly random experiment, the values of probability of detection and probability of false alarm determined by the trigger box guide the selection of the number of trials. Of course in terms of the design of a Monte Carlo experiment, the number of trials also governs the precision of the resulting estimates of probability of detection and probability of false alarm. Therefore, having an analytical solution of the ROC curve, for a give SNR is valuable. The ROC curve shown in Figures 3 and 4 is used in this experiment. From a data logging perspective, it is desirable to construct arrays that are large enough that meaningful histograms can be derived from them.

With assuming the least about the a priori probabilities, maximum entropy is employed by the use of uniform density functions for trial generations. For a truly random experiment, this means that whether a signal is present along with the Gaussian noise is determined by a binary-uniform-random-number generator. Thus for each trial, there is an equally likely chance that a signal is or is not present along with the noise. If a signal is present, the value of the TEC parameter associated with that signal is generated by a random number generator that has a continuous uniform distribution for all valid values of TEC. Of course the noise component of every signal is generated by a normally-distributed, continuous random number generator.

For this paper the parameters of both the simulation and the Monte Carlo experiment were selected for computing feasibility and plausibility of the scenario. The signal to noise ratio associated with each channel of the analog trigger box, was selected to be 3dB. Examining the ROC curve of the analog trigger box, the detection point 2-of-8 channels detects was chosen to be used in this paper. Thus the binary threshold is set at 2 and the individual channel thresholds are determined via the Harrington's method [6]. The number of trials was set to 100,000. This number of trials should yield enough logged false alarms to construct a meaningful histogram.

4. THRESHOLD DETERMINATION

The Monte Carlo experiment provides the data needed to approximate the relevant pdfs (probability density functions) needed for the determination of the thresholds. For each of the algorithms, data was collected during the experiment that recorded the value of the estimated TEC or correlation peak for the case of detect and for the case of a false alarm. The conditions of detect and false alarm refer to the decision being solely made by the trigger box. These data can now be used to compute normalized histograms that estimate conditional probability density functions. Two conditional pdfs are computed for each algorithm; the probability of estimated TEC (or correlation peak) value given true detection, $p(\mathrm{TEC} \mid D)$ and the probability of estimated TEC (or correlation peak) value given a false alarm, $p(\mathrm{TEC} \mid FA)$. Under Bayes' Detection and the Min-Max Criterion were all cost are the same, the two conditional pdfs are the likelihood functions that populate the decision space.

Relative positioning of the conditional pdfs in the decision space will determine what can be achieved by implementing detection thresholds in the space. Reduction in the probability of false alarms may come at the cost of a reduction in probability of detection. In fact this cost in probability of detection is the case for all the algorithms except the MF algorithm. For the first three algorithm, the $p(\mathrm{TEC} \mid D)$ is girdled by $p(\mathrm{TEC} \mid FA)$. This relationship between two likelihood functions is different than what is usually dealt with in signal detection texts. In most texts on the subject the likelihood functions have a relationship of "overlapping tails" in the decision space. Still the with some scarifies of probability of detection, the relationship of one likelihood function girdled by another that spans a large range of the decision space can be used to reduce the probability of false alarm.

The methodology for determination of the threshold values in the decision space is presented. First an acceptable loss in probability of detection most be specified. For this paper an acceptable absolute loss in probability of detection is 4%. Once a loss is specified, the area underneath the likelihood function condition on detection can be determined by subtracting the ratio of the specified probability of detection loss to the current probability of detection from one.

$$Area\ under\ p(TEC \mid D) = 1 - \frac{\text{Specified Loss}}{P_D}$$

With the area derived, two thresholds in the decision space must be determined so that in between the two thresholds the area underneath $p(\text{TEC} \mid D)$ is equal to the area derived from the specified loss in probability of detection. With the above being a condition and the reasonable condition that the thresholds must include the full range of legitimate values for TEC, $5\times10^{16} \le TEC \le 5\times10^{18}$, thresholds can be initially placed. At this point the rough placement of the thresholds can be determined by the used of autonomous algorithm.

The autonomous algorithm used in this paper assumed an approximately symmetric, uni-modal likelihood function to determine thresholds. Since the likelihood function of $p(\text{TEC} \mid D)$ is assumed to be uni-modal, the first step in the algorithms was to find the maximum value of the function. From the maximum-value abscissa location, the needed area underneath the function is determined by expanding on both sided along the abscissa in manner so that one threshold is approximately the same distance from the mode as the other threshold. The first condition of required area is met in this way. Next both thresholds are evaluated for compliance to constraints of the problem.

The assumption of a uni-modal likelihood function lacks validity to some extend, thus the thresholds derived from the assumption must be examined and, if necessary, adjusted to comply with the constraints of the problem. In the ideal case, the Monte Carlo experiment of this paper would have yielded a likelihood function that is a uniform pdf with limits that are the valid values of TEC. However, the parameter estimation algorithms are not ideal, so outlying estimates exist and the profile of the pdf can not be assumed to be uniform. The resulting thresholds must be examined to make sure that all valid values of TEC are inclusive. If not the threshold values are shifted so as to include the valid values and still maintain the desired area of the function. As an example, this adjustment may involve shifting both thresholds to the left or right by an equal number of abscissa bins. Clearly the final selection of the threshold values has a heuristic component to it. The result is threshold values related to TEC estimation that are sensible and should result in a decrease in the probability of false alarm.

The derived thresholds now can be used to calculate an estimate of resulting probability of false alarm due to post processing of the results from the parameter estimation algorithm. For the Monte Carlo experiment the conditional pdf of $p(\text{TEC} \mid FA)$ is utilized. The area under the conditional pdf between the two thresholds is calculated to determine the resulting probability of false alarm. With post processing of results from the parameter estimation algorithm, new detection criteria can be imposed and the resulting performance can be estimated.

4.1 Example Calculation

Decisions about the validity of the results from the exercising of the least-mean-squares algorithm have to be made before the pdfs can be constructed. The number of valid detections processed by the LMS algorithm was 28,003 and the number of false alarms processed was 3658. These numbers are the same for all four algorithms since they are determined by the performance of the analog trigger box simulation. Under the constraints of the experiment these number yield a probability of detection of 55% and probability of false alarm of 7.3% for the analog trigger box. These numbers are close to analytical predictions of 53% for probability of detection and 4.7% for probability of false alarm. What different there is between the Monte Carlo results and the analytical results are most likely due to assumptions made in deriving the analytical solution [6]. The results from the Monte Carlo simulation can be considered valid.

In order to determine detection thresholds for the results of the LMS parameter estimation algorithm, two conditional pdfs must be constructed. There are 28,003 estimated TEC values available for the construction of the $p(\text{TEC} \mid D)$ and 3658 values available for the construction of the $p(\text{TEC} \mid FA)$. Histograms will be used to construct estimates of the two conditional probability density functions. After some investigation it was determined that 500 bins would be used to construct all histograms. Figure 5 shows the histogram estimates of the two conditional pdfs. Shown in the figure are to overlapping uni-modal pdfs.

Setting of the detection-acceptance thresholds involves integrating area under the two curves. First thresholds are set so that area under pdf conditioned on detect relates to an overall loss of detection performance of 4%, which corresponds to a conditional pdf area of 99.93%. For the most part this area is defined by symmetrically expanding from the mode. The associated probability of false alarm can then be estimated from the area of the pdf conditioned on false alarms that is defined by the two thresholds. The amount of probability defined by this area is used to scale the value of probability of false alarm due solely to the analog trigger box.

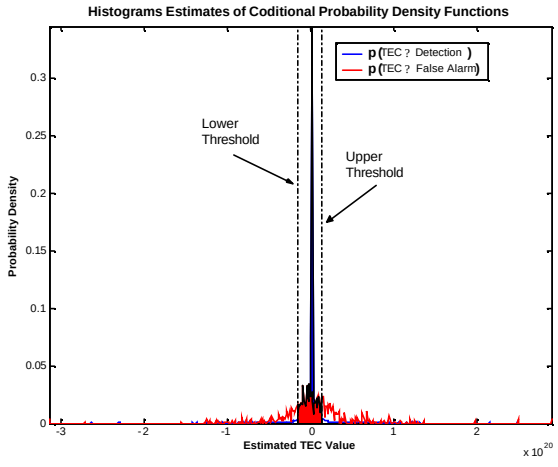

Figure 5. Histogram Estimates of Conditional Probability Density Functions for LMS Algorithm

4.2 Thresholds and Estimated Performance

An examination and analysis of all the results from the Monte Carlo experiment yielded the following thresholds for the four parameter-estimation algorithms.

Table 1. Thresholds for Parameter Estimation Algorithms

Algorithm	Left Threshold	Right Threshold
Least Mean Squares	-1.9913e19 (e^-/m^2)	1.0553e19 (e^-/m^2)
Maximum Likelihood	-8.8654e18 (e^-/m^2)	5e18 (e^-/m^2)
Software Trigger Box	5e16 (e^-/m^2)	5e18 (e^-/m^2)
Match Filter Bank	137.2017 (peak number)	Infinity (peak number)

Performance estimates about the four algorithms and their associated thresholds presented in Table 1, can be made with some analysis. First the area between the thresholds for both of the pdfs must be determined. This operation will provide two values of probability that can be used to scale the probability of detection and probability of false alarm associated with the analog trigger box. Table 2 gives the resulting estimates of performance for the four algorithms based on this procedure.

Table 2. Prediction in Detection Performance

Algorithm	Probability of Detection	Probability of False Alarm
Least Mean Squares	51.26%	3.55%
Maximum Likelihood	50.58%	3.61%
Software Trigger Box	50.81%	2.90%
Match Filter Bank	51.25%	4.06e-003%

One point to note is that the probability of detection for the MF algorithm could have been increased since only the $p(\mathrm{TEC} \mid D)$ is present at the left threshold value. The figure below shows the relationship of the two conditional pdfs.

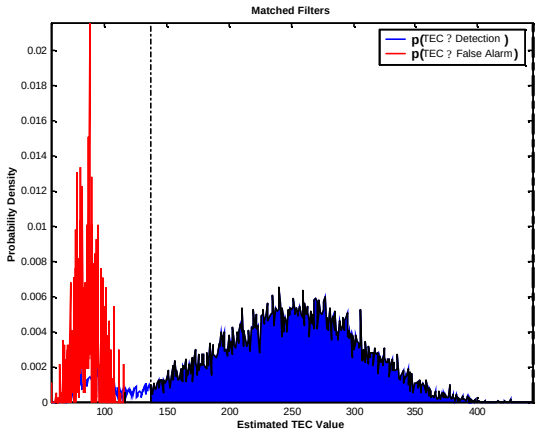

Figure 6. Histogram Estimates of Conditional Probability Density Functions for MF Algorithm

5. VALIDATION EXPERIMENT

In order to valid the concept of using the parameter estimation algorithms to improve detection performance, another hundred thousand trial Monte Carlo experiment was performed. This experiment made use of the calculated thresholds to test the detection validity of each trial. Of course since the true nature of each signal is know, detection performance numbers can be determined for each algorithm. The results of the experiment are shown in Table 3. The experiment result for the probability of detection of the analog trigger box was 54.86% and its probability of false alarm was 7.25%.

Table 3. Monte Carlo Results for Detection Performance

Algorithm	Probability of Detection	Probability of False Alarm
Least Mean Squares	50.75%	3.58%
Maximum Likelihood	50.75%	3.74%
Software Trigger Box	52.60%	2.01%
Match Filter Bank	50.79%	0

6. RESULTS

From the results of the validation experiment, a difference between the four algorithms is present. False alarms are reduced most dramatically by the match-filter bank algorithm. They were reduced to a level below what could be determined by the Monte Carlo experiment where 50-thousand opportunities were presented. The software trigger box algorithm provided the second greatest reduction in false alarms by nearly a factor of 4 better than the analog trigger box. The least-mean squares and maximum likelihood algorithms performed approximately the same and provide the least improvement of the four algorithms. Roughly a factor of two decrease in probability of false alarm is

achieved by the post-processing of the results of these two parameter estimation algorithms.

The correlation of these results with each algorithms energy usages is presented in the figure below. A general relationship can be stated that the more energy that is expended, the greater the reduction in the probability of false alarm.

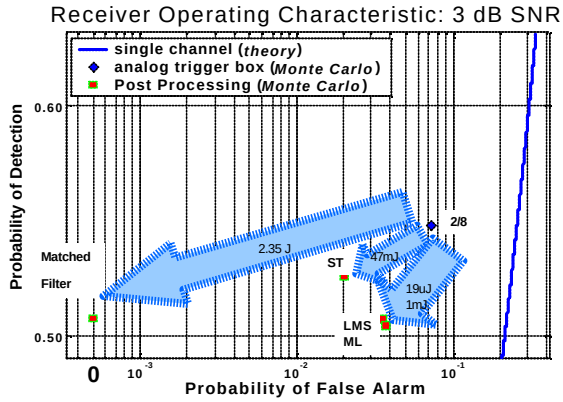

Figure 7. Detection performance improvement shown on ROC curve with associated energy usage.

Figure 8 shows the relationship between energy usage and probability of false alarm performance. Ignoring the ML-labeled point, the graph shows that several orders in magnitude of energy (expended) are needed for a meaningful improvement in probability of false alarm. However, it does show that with enough energy, the false alarm probability can be made zero (or close to zero).

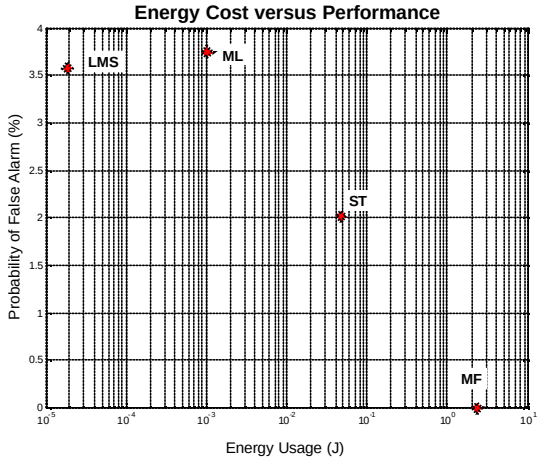

Figure 8. Energy Cost versus Probability of False Alarm for the Four Post-Processing Algorithms

7. CONCLUSIONS

The work presented in this paper shows that *in situ* parameter estimation algorithms can be used to improve detection performance, or more precisely reduce the probability of false alarm. Thus post-processing of data can yield improvements in detection performance. Also, this work shows that the cost of this reduction in probability of false alarm can be measured in energy usage. In fact for the case presented in this paper, orders of magnitude more energy needs to be expended to produce significant reductions in false alarms. One point that should be noted is that the information must be available in the data provide for any expenditure of energy to be of value.

Information availability could be the reason two of the algorithms reduced probability of false alarm near equally. Both the LMS and ML algorithms use only the data provide by the analog trigger box. However, the two algorithms require different usages of energy. The difference in energy is by a factor of approximately 50, which is very significant. These relationships could be explained in terms of information content. That is all the available information for the improvement of false alarms contained in the data that was provided was exhausted by the LMS algorithm. There may be no unused information for the ML algorithm to reduce the probability of false alarm than what was accomplished by the LMS algorithm. This leads to the conclusion that if the information is not present, no amount of energy expended in post processing will improve detection performance.

8. ACKNOWLEDGMENTS

This effort is sponsored by the Defense Advanced Research Projects Agency (DARPA) through the Air Force Research Laboratory, USAF, under agreement number F30602-00-2-0548. We are indebted to JPL for the use of their Power PC testbench to measure algorithm power usage, and thanks specifically to Jeffrey Mankung of JPL for his invaluable assistance with the testing.

9. REFERENCES

[1] DARPA Power-Aware Computing and Communications http://www.darpa.mil/ipto/research/PAC/C/index.htm

[2] Shriver, Patrick M., Maya B. Gokhale, et al., "A Power-Aware, Satellite-Based Parallel Signal Processing Scheme," Power Aware Computing. Eds. Robert Graybill and Rami Melhem. New York: Kluwer Academic/Plenum Publishers, 2002. Ch. 13: 243-259.

[3] Los Alamos National Laboratory Fast On-orbit Recoding of Transient Events Project (FORTÉ) http://www.FORTÉ.lanl.gov/nis-projects/FORTÉ/intro.html

[4] Enemark, D. C., and Shipley, M. E. The FORTÉ receiver and sub-band triggering unit. In 8th Annual AIAA/Utah State University Conference on Small Satellites. 1994.

[5] Roussel-Dupré, D., Klinger, P., et al. (2001). "Four Years of Operations and Results with FORTÉ." Proceedings of the AIAA Space 2001 Conference. AIAA 2001-4627

[6] DiFranco, J.V., and Rubin, W.L. Radar Detection, Artech House, Dedham, MA, 1980. Chapter 14.

[7] Press, W., et al. Numerical Recipes in C, 2nd edition. Cambridge University Press., 1992, pages 699-705.